

## $\Delta$ degrees of freedom in trinuclei. II. The Hannover $\Delta\Delta$ model

A. Picklesimer

*Physics Division, Los Alamos National Laboratory, Los Alamos, New Mexico 87545*

R. A. Rice

*Physics Division, Los Alamos National Laboratory, Los Alamos, New Mexico 87545  
and Department of Physics, Purdue University, West Lafayette, Indiana 47907*

R. Brandenburg

*Physics Division, Los Alamos National Laboratory, Los Alamos, New Mexico 87545  
and Institute for Physics, University of Basel, 3056 Basel, Switzerland*

(Received 16 September 1991)

The effect of  $\Delta$  and  $\Delta\Delta$  degrees of freedom on the triton binding energy ( $E_T$ ) is studied using the Hannover  $\Delta\Delta$  force model. The three-body system of interest extends through  $J \leq 4$ , with  $L(N\Delta), L(\Delta\Delta) \leq 4$ . A series of preliminary investigations reduces this three-body problem to  $J \leq 2$ , with  $L(N\Delta), L(\Delta\Delta) \leq 2$ , and a 110 keV attractive correction to  $E_T$ . These  $J \leq 2$   $\Delta\Delta$  calculations reveal a repulsive dispersive effect of 930 keV and an attractive  $\Delta\Delta$  three-body force effect of 500 keV, in addition to the corresponding one- $\Delta$  effects of 550 and 920 keV, respectively. The total  $\Delta$ -induced dispersive effect is thus about 1480 keV, while the total  $\Delta$ -induced three-body force effect is about 1420 keV:  $\Delta$  effects on  $E_T$  almost exactly cancel. The net  $\Delta\Delta$   $J \leq 2$  result is  $E_T = 7.32$  MeV, while the corresponding nucleons-only result is 7.38 MeV. Similarly, the net  $J \leq 4$  result is  $E_T = 7.43$  MeV, as compared to the corresponding nucleons-only result, 7.46 MeV. The Hannover  $\Delta\Delta$  force model is also examined for consistency with the two-body scattering parameters and is found to be somewhat defective in this regard. Thus, the important implications of these qualitative results for nuclear physics are to some extent dependent on confirmation using more sophisticated force models.

PACS number(s): 21.45.+d, 21.10.Dr, 21.30.+y, 27.10.+h

### I. INTRODUCTION

This paper investigates the triton binding energy ( $E_T$ ) in a model which allows  $\Delta$  excitations of the nucleon to appear explicitly in the bound state. The calculations are based on a coupled-channel approach in which a potential interaction allows transitions between the nucleon and  $\Delta$  intrinsic states. The  $\Delta$  is treated as a stable particle with the quantum numbers of the  $\Delta$  isobar and a mass of 1236 MeV. The previous paper in this series [1] reported the results of calculations in which the  $\Delta$  content of the triton was restricted to a single  $\Delta$ , and which used the Hannover one- $\Delta$  force model [2]. There the attractive one- $\Delta$  three-body-force (3BF) contribution was found to be largely offset by the repulsive dispersive effect induced by the  $\Delta$  in the nucleon-nucleon ( $NN$ ) sector, in agreement with the results found earlier by the Hannover group [2]. Here the investigations are extended to study  $\Delta\Delta$  degrees of freedom in the triton as well, using the Hannover  $\Delta\Delta$  force model [3].

In the more usual approach to the triton problem which uses only nucleon degrees of freedom,  $NN$  potentials must be augmented by three-nucleon ( $NNN$ ) potentials in order to reproduce the physical binding energy. These latter are based on diagrams such as the one depicted in Fig. 1 and assume that only one nucleon resonance is present at a time. Clearly, the adequacy of such an approach depends crucially on the assumption that

the probability of finding more than one nucleon resonance in the triton simultaneously is small. If this probability is not small enough, then a much more complicated set of diagrams is necessary to represent the  $NNN$  potential.

A further calculation by the Hannover group [3], extended to include (perturbatively)  $NN-\Delta\Delta$ ,  $N\Delta-\Delta\Delta$ , and  $N\Delta-\Delta N$  potential amplitudes in the triton, found that the additional dispersive effect attributable to this extension of the model was very large (larger than the corresponding effect of the original single  $\Delta$  model) and was not balanced by the additional 3BF contribution (which was an order of magnitude smaller than the effect in the one- $\Delta$  model). The conclusions drawn from these results were that (1) dispersive effects dominate over three-body force

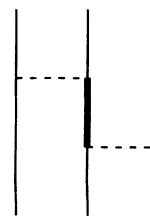


FIG. 1. Typical three-body-force diagram. The thin lines represent nucleons in their intrinsic state, and thick lines stand for a nucleon resonant state. The dashed lines represent exchange mesons.

effects in the net  $\Delta$  contribution to  $E_T$ , so that (2) the inclusion of  $\Delta$  degrees of freedom worsens the theoretical defect in  $E_T$  seen in nucleons-only models by about a factor of 2, leaving the triton grossly underbound, and (3) that this evidence for the dominance of dispersive effects seems conclusive because the attractive 3BF contribution to  $E_T$  from  $\Delta$  configurations converges rapidly with the number of  $\Delta$  excitations, and is in fact well represented by single- $\Delta$  excitation. It was, however, further found that the percentage of  $\Delta\Delta$  amplitudes in the triton wave function is, at 5%, relatively large. Although as emphasized by the authors of Ref. [3] this investigation was exploratory (among other things, the neglect of  $\Delta\Delta$ - $\Delta\Delta$  potential amplitudes is worrisome), the implications of their results for the triton, and for nuclear physics in general, are profound. Thus, it is necessary to examine more carefully the implications of the  $\Delta$  degrees of freedom of the Hannover  $\Delta\Delta$  model [3] and, in particular, to remove the limitations inherent in the perturbative calculations of Ref. [3].

This is the motivation of the current work. The work reported here employs the Hannover  $\Delta\Delta$  force model as defined in Ref. [3], and includes both  $\Delta$  and  $\Delta\Delta$  degrees of freedom in a comprehensive, nonperturbative analysis. As will be seen, the conclusions of this work differ greatly from those of Ref. [3], yielding an entirely different pic-

ture of the physical implications of  $\Delta$  degrees of freedom. The extended Hannover potential model will be referred to throughout as the Hannover  $\Delta\Delta$  model. However, the reader is cautioned that since an  $N\Delta$ - $\Delta N$  potential amplitude forms part of the extension of the original Hannover one- $\Delta$  model, differences between the  $\Delta\Delta$  and one- $\Delta$  models are not entirely due to  $\Delta\Delta$  effects, but also reflect this additional one- $\Delta$  component. No attempt is made to disentangle the effects of this additional one- $\Delta$  component.

The next section gives a synopsis of the three-body equations needed for the subsequent discussion of the results. A review of the Hannover  $\Delta\Delta$  force model is given in Sec. III, including a comparison between the two-body properties that it predicts and those of the Paris potential, while Sec. IV presents the main results of this paper. The final section briefly summarizes the results, their implications, and further issues which remain to be addressed.

## II. FORMALISM

This section summarizes the Faddeev equations which are solved to obtain the triton binding energy and wave function, for the case where  $\Delta$  degrees of freedom are included. The Faddeev equations take the form

$$\Psi(pq\alpha) = \sum_{\bar{\gamma}} \sum_{\alpha'} \int_0^\infty dq' q'^2 \int_{-1}^1 dx' t_{\gamma\bar{\gamma}}^{JT}(p, p_1; E, q, n_z) G_0(E, q', p_2; n'_z, N'_z) G_{\bar{\alpha}, \alpha'}(q, q', x') \Psi(p_2, q', \alpha'). \quad (1)$$

Here the functions  $\Psi$ ,  $t$ ,  $G_0$ , and  $G$  are the Faddeev amplitudes, the two-body  $t$  matrices, the free three-body Green's function, and the geometrical coefficient, respectively. The variables  $p$  and  $q$  are the Jacobi variables for the pair and spectator momentum, respectively, and  $E$  is the total energy of the three-body system,  $E = M_T c^2$ . The variable  $\alpha$  represents all of the quantum numbers necessary to specify the three-body amplitude, and is given by

$$\alpha = \{[(LS)J, (ls(n_z))j] \mathcal{J} \mathcal{J}_z; (Tt(n_z)) \mathcal{T} \mathcal{T}_z; NN_z, \frac{1}{2} n_z\}. \quad (2)$$

The convention used here is that lower-case, upper-case, and script letters denote the pair, spectator, and total quantum numbers, respectively. The variable  $\gamma$  is used to represent the set of pair quantum numbers in which the potential interaction need not be diagonal:

$$\gamma = \{LSNN_z\}. \quad (3)$$

The quantities  $x'$ ,  $p_1$ , and  $p_2$  are given by

$$x' = \frac{\mathbf{q} \cdot \mathbf{q}'}{qq'}, \quad (4)$$

$$p_1^2 = \left[ \frac{m(n'_z)}{M(\bar{N}_z)} \right]^2 q^2 + q'^2 + 2 \left[ \frac{m(n'_z)}{M(\bar{N}_z)} \right] qq' x', \quad (5)$$

and

$$p_2^2 = q^2 + \left[ \frac{m(n_z)}{M(N'_z)} \right]^2 q'^2 + 2 \left[ \frac{m(n_z)}{M(N'_z)} \right] qq' x', \quad (6)$$

where  $m(n_z)$  and  $M(N_z)$  are the masses of the spectator and "pair," respectively. The quantum numbers  $n$  and  $N$ , and their corresponding  $z$  components, are the "n-spin" quantum numbers introduced in Ref. [1] to denote the nucleon/delta content of the state, and are defined such that

$$n_z = \begin{cases} -\frac{1}{2} & \text{nucleon,} \\ +\frac{1}{2} & \text{delta,} \end{cases} \quad (7)$$

$$N_z = \begin{cases} -1 & NN, \\ 0 & N\Delta, \\ +1 & \Delta\Delta. \end{cases} \quad (8)$$

For a more detailed description of the notation and conventions, the Faddeev equations and the functions  $t$ ,  $G_0$ , and  $G$ , appropriate for the case where  $\Delta$  degrees of freedom are explicitly allowed, the reader is referred to Ref. [1], especially Sec. II and Appendixes A and B. Similarly, Appendix C of Ref. [1] details the methods used to check our computational machinery in the one- $\Delta$  case. Because of the parallel structure of the Hannover one- $\Delta$  and  $\Delta\Delta$  interactions (see Refs. [1–3] and the next section), and especially because the computer coding is

largely blind to the distinction between no- $\Delta$ , one- $\Delta$ , and  $\Delta\Delta$  channels, [1] the checking in Ref. [1] validates most of the computational machinery used in the  $\Delta\Delta$  calculations of this paper as well. Also due to the parallel structure of the interactions, only minor extensions of the two-body codes were required to include  $\Delta\Delta$  channels. The only significant extension was to the Hannover “renormalization” scheme (see the next section) and this was cross-checked with the  $t$ -matrix code using simple extensions (turning interactions involving  $\Delta$  sectors on and off) of the  $V_{\text{eff}}$  and renormalization point methods described in Appendix C of Ref. [1].

### III. FORCE MODEL

The force model used in this work is the Hannover  $\Delta\Delta$  model. This model includes interactions between all of the two-body  $NN$ ,  $N\Delta$ , and  $\Delta\Delta$  channels, except for the diagonal  $\Delta\Delta$  interaction which is set to zero. The two-body diagrams involving  $\Delta$ 's which are included in the Hannover  $\Delta\Delta$  model are shown in Fig. 2 (the diagonal  $NN$  and adjoint diagrams are not shown). Note that the diagonal  $N\Delta$  interaction is defined solely in terms of the  $N\Delta$  exchange diagram of Fig. 2(b); the nonexchange potential is set to zero. This model is a simple extension of the Hannover one- $\Delta$  model [2], and was defined by the Hannover group [3] through the introduction of the  $N\Delta$  exchange potential of Fig. 2(b) and the potential amplitudes which connect  $\Delta\Delta$  states to  $NN$  and  $N\Delta$  states. The  $\Delta\Delta$  model potentials which involve  $\Delta$ 's contain contributions from both  $\pi$  and  $\rho$  exchanges, given by

$$\langle \mathbf{p} | V_{\pi} | \mathbf{p}' \rangle = - \frac{1}{(2\pi\hbar)^3} \frac{f_{\pi}(1)f_{\pi}(2)}{m_{\pi}^2 c^4} \frac{\Lambda^2 - m_{\pi}^2 c^2}{\Lambda^2 + (\mathbf{p} - \mathbf{p}')^2} \times \mathbf{t}_1 \cdot \mathbf{t}_2 \frac{\mathbf{s}_1 \cdot (\mathbf{p} - \mathbf{p}') \mathbf{s}_2 \cdot (\mathbf{p} - \mathbf{p}')}{m_{\pi}^2 c^2 + (\mathbf{p} - \mathbf{p}')^2}, \quad (9)$$

$$\langle \mathbf{p} | V_{\rho} | \mathbf{p}' \rangle = - \frac{1}{(2\pi\hbar)^3} \frac{f_{\rho}(1)f_{\rho}(2)}{m_{\rho}^2 c^4} \frac{\Lambda^2 - m_{\rho}^2 c^2}{\Lambda^2 + (\mathbf{p} - \mathbf{p}')^2} \times \mathbf{t}_1 \cdot \mathbf{t}_2 \frac{[\mathbf{s}_1 \times (\mathbf{p} - \mathbf{p}')] \cdot [\mathbf{s}_2 \times (\mathbf{p} - \mathbf{p}')] }{m_{\rho}^2 c^2 + (\mathbf{p} - \mathbf{p}')^2}, \quad (10)$$

where the coupling constants  $f_{\pi}(i)$  and  $f_{\rho}(i)$  and the spin and isospin operators  $\mathbf{s}_i$  and  $\mathbf{t}_i$  are chosen according to the character of the vertex  $i$  in the corresponding potential diagram. The appropriate choices of the coupling constants and the spin and isospin operators for the four diagrams of Fig. 2 are given in Table I. The potentials

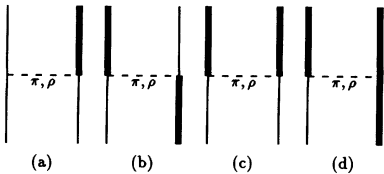


FIG. 2. The two-body potential diagrams involving  $\Delta$ 's which are included in the Hannover  $\Delta\Delta$  model (adjoint diagrams are not shown).

corresponding to other diagrams are obtained by permuting the vertex indices 1 and 2 or by taking the Hermitian adjoint of the forms in Eqs. (9) and (10) as appropriate. Numerical values for the coupling constants, meson masses, and cutoff mass used in this work are given in Table II. Here, as in Ref. [1], the  $N$  and  $\Delta$  masses are taken to be 938.93 and 1236 MeV, respectively. Expressions useful for the calculation of the partial-wave matrix elements of the various operators appearing in Eqs. (9) and (10) can be found in Refs. [1,4]. As in the case of the Hannover one- $\Delta$  model, the  $\Delta\Delta$  model is constructed as an extension of the Paris  $NN$  potential [5].

The partial-wave potential matrix elements employed in the calculations are of the form

$$\langle p, (LS)JJ_z; TT_z; NN_z | V | p', (L'S')J'J'_z; T'T'_z; N'N'_z \rangle = V_{\gamma, \gamma'}^{JT} (p, p') \delta_{JJ'} \delta_{J_z J'_z} \delta_{TT'} \delta_{T_z T'_z}, \quad (11)$$

where  $\gamma$  denotes the set of two-body quantum numbers defined in Eq. (3). Since in this section the discussion centers on the nucleon/delta content of the two-body states, the potential amplitudes will be characterized by the quantum numbers  $N_z, N'_z$  of Eq. (8) through the notation  $V_{N_z, N'_z}$ , all other quantum numbers being suppressed for convenience. The potentials introduced in the extension to the Hannover  $\Delta\Delta$  model are in this notation  $V_{-1,1}$ ,  $V_{0,0}$ , and  $V_{0,1}$ .

In extending the one- $\Delta$  model, the original Hannover diagonal  $NN$  potential ( $V_{-1,-1}$ ) needs to be “renormalized” due to the coupling to the  $\Delta\Delta$  states. This is done in analogy to the renormalization procedure used in Ref. [2], and the result is [3]

$$V_{-1,-1} = V_p - V_{-1,0} g_0(E_r) V_{0,-1} - V_{-1,1} g_0(E_r) V_{1,-1}. \quad (12)$$

Here  $V_p$  is the Paris [5]  $NN$  potential and  $g_0(E)$  is the two-body Green's function

$$g_0(E) = \frac{1}{E - h_0}, \quad (13)$$

with  $h_0$  the free two-particle Hamiltonian and  $E$  the energy, both including the rest-mass energies of the particles. In the  $\Delta\Delta$  model, the diagonal  $N\Delta$  potential ( $V_{0,0}$ ) which results from the diagram of Fig. 2(b) must also be renormalized. The added renormalization term is [3]

$$- V_{0,1} g_0(E_r) V_{1,0}. \quad (14)$$

The choice of the renormalization energy  $E_r$ , which corresponds to that taken in Ref. [3] and which is consistent with the definition of  $h_0$  used here is

$$E_r = \begin{cases} M_D c^2 & J^\pi, T = 1^+, 0, \\ 2M_N c^2 & \text{otherwise,} \end{cases} \quad (15)$$

where  $\pi$  denotes parity;  $M_D$  and  $M_N$  are the rest mass of the deuteron and the nucleon, respectively.

The purpose of the renormalization is to approximately preserve the low-energy two-nucleon properties obtained

TABLE I. Appropriate choices for the coupling constants and the spin and isospin operators which appear in Eqs. (9) and (10) for the four diagrams of Fig. 2. The operator  $\sigma$  is the spin operator in the spin- $\frac{1}{2}$  representation with reduced matrix element [9]  $(\frac{1}{2}||\sigma||\frac{1}{2})=\sqrt{6}$ ,  $\mathbf{S}$  is the  $\frac{1}{2}$  to  $\frac{3}{2}$  spin transition operator with reduced matrix element  $(\frac{3}{2}||\mathbf{S}||\frac{1}{2})=2$ , and  $\Sigma$  is the spin operator in the spin- $\frac{3}{2}$  representation with reduced matrix element  $(\frac{3}{2}||\Sigma||\frac{3}{2})=2\sqrt{15}$ , with parallel definitions for the isospin operators  $\tau$ ,  $\mathbf{T}$ , and  $\Theta$ , respectively.

Diagram	$f_{\pi}(i)$		$f_{\rho}(i)$		$\mathbf{s}_i$		$\mathbf{t}_i$	
	$i=1$	$i=2$	$i=1$	$i=2$	$i=1$	$i=2$	$i=1$	$i=2$
(a)	$f_{\pi NN}$	$f_{\pi N\Delta}$	$f_{\rho NN}$	$f_{\rho N\Delta}$	$\sigma$	$\mathbf{S}$	$\tau$	$\mathbf{T}$
(b)	$f_{\pi N\Delta}$	$f_{\pi N\Delta}$	$f_{\rho N\Delta}$	$f_{\rho N\Delta}$	$\mathbf{S}$	$\mathbf{S}^\dagger$	$\mathbf{T}$	$\mathbf{T}^\dagger$
(c)	$f_{\pi N\Delta}$	$f_{\pi N\Delta}$	$f_{\rho N\Delta}$	$f_{\rho N\Delta}$	$\mathbf{S}$	$\mathbf{S}$	$\mathbf{T}$	$\mathbf{T}$
(d)	$f_{\pi N\Delta}$	$f_{\pi\Delta\Delta}$	$f_{\rho N\Delta}$	$f_{\rho\Delta\Delta}$	$\mathbf{S}$	$\Sigma$	$\mathbf{T}$	$\Theta$

from the Paris  $NN$  potential. In the Hannover one- $\Delta$  model, the renormalization scheme ensured that at the renormalization energy,  $E_r$ , the  $NN$ - $NN$   $t$ -matrix amplitudes reproduced *exactly* the  $t$ -matrix amplitudes predicted by the Paris potential (in the one- $\Delta$  model,  $E_r=2M_Nc^2$ ). In the extended  $\Delta\Delta$  model with the renormalization as given above, this is *not* the case. Only for the isospin  $T=0$  amplitudes, to which  $N\Delta$  states cannot couple, is the  $NN$ - $NN$   $t$ -matrix amplitude at the renormalization energy exactly the same as given by the Paris potential. For the isospin  $T=1$  amplitudes, including the important  $^1S_0$  state, the above renormalization is not exact, even at  $E_r$ .

This can be seen most easily by considering the effective, energy-dependent potential  $V_{\text{eff}}(E)$  defined by

$$\begin{aligned}
V_{\text{eff}}(E) &= V_{-1,-1} \\
&+ [V_{-1,0} + V_{-1,1}g_0(E)V_{1,0}]g_1(E)V_{0,-1} \\
&+ [V_{-1,1} + V_{-1,0}g'(E)V_{0,1}]g_2(E)V_{1,-1},
\end{aligned} \tag{16}$$

where

$$g_1(E) = [E - h_0 - V_{0,0} - V_{0,1}g_0(E)V_{1,0}]^{-1}, \tag{17}$$

$$g_2(E) = [E - h_0 - V_{1,0}g'(E)V_{0,1}]^{-1}, \tag{18}$$

and

$$g'(E) = (E - h_0 - V_{0,0})^{-1}. \tag{19}$$

This effective  $NN$  potential is defined to reproduce, in a

TABLE II. Values of the potential parameters as used in this work.

Parameter	Value
$f_{\pi NN}^2/4\pi$	0.08
$f_{\pi N\Delta}^2/4\pi$	0.35
$f_{\pi\Delta\Delta}^2/4\pi$	0.0032
$f_{\rho NN}^2/4\pi$	5.20
$f_{\rho N\Delta}^2/4\pi$	22.8
$f_{\rho\Delta\Delta}^2/4\pi$	0.208
$m_{\pi}c^2$	138.0 MeV
$m_{\rho}c^2$	760.0 MeV
$\Lambda c$	1.2 GeV

calculation with only nucleon degrees of freedom, exactly the same  $NN$   $t$ -matrix amplitudes as are obtained in a coupled-channel calculation including explicit  $\Delta$  degrees of freedom using the Hannover  $\Delta\Delta$  model potentials  $V_{-1,-1}$ ,  $V_{-1,0}$ ,  $V_{-1,1}$ ,  $V_{0,1}$ ,  $V_{0,0}$ , and their Hermitian adjoints.

Now it is easy to define the  $NN$ - $NN$  potential  $V_{-1,-1}$  as the desired renormalization of the Paris potential. One simply has

$$\begin{aligned}
V_{-1,-1} &= V_P \\
&- [V_{-1,0} + V_{-1,1}g_0(E_r)V_{1,0}]g_1(E_r)V_{0,-1} \\
&- [V_{-1,1} + V_{-1,0}g'(E_r)V_{0,1}]g_2(E_r)V_{1,-1},
\end{aligned} \tag{20}$$

so that at the renormalization energy,  $V_{\text{eff}}(E_r) \equiv V_P$ . This guarantees that the  $NN$ - $NN$   $t$ -matrix amplitude at this energy is exactly that of the Paris potential. In a recent one- $\Delta$  study which includes a diagonal  $N\Delta$  potential, the Hannover group used a method similar to the above for renormalizing their  $NN$  potential [6]. The generalization of the above discussion for the case where the  $\Delta\Delta$ - $\Delta\Delta$  potential,  $V_{1,1}$ , is nonzero, is also straightforward.

The renormalized potential of Eq. (20) simplifies for  $T=0$ , where there is no coupling to  $N\Delta$  channels, to

$$V_{-1,-1} = V_P - V_{-1,1}g_0(E_r)V_{1,-1}. \tag{21}$$

This is the same as Eq. (12) for isospin  $T=0$  amplitudes, so that the renormalization employed in the Hannover  $\Delta\Delta$  model does result in the reproduction of the deuteron binding energy in the  $^3S_1$ - $^3D_1$   $NN$  channels ( $E_r = M_Dc^2$ ) and the  $t$  matrices at the scattering threshold ( $E_r = 2M_Nc^2$ ) in the other  $T=0$   $NN$  channels. For isospin  $T=1$ , the Hannover  $\Delta\Delta$  renormalization of Eqs. (12) and (14) is only an approximation to that of Eq. (20), so that the Hannover  $NN$   $t$  matrices will not be identical to those predicted by the Paris potential, even at the renormalization energy  $E_r$ . Due to this approximate nature of the renormalization, the Hannover  $\Delta\Delta$  model turns out to be somewhat problematical, since, for example, it performs relatively poorly in reproducing the  $^1S_0$  two-body scattering parameters and phase shifts.

The fact that  $E_r$  is chosen to be  $M_Dc^2$  in the  $^3S_1$ - $^3D_1$   $NN$  partial waves ensures that the model reproduces ex-

actly the deuteron binding energy calculated from the Paris potential alone,  $E_D = 2.2249$  MeV. However, the deuteron itself differs from that of the Paris potential by the presence of  $\Delta\Delta$  components and by the consequent adjustment to the normalization of the  $NN$  component. The performance of the Hannover  $\Delta\Delta$  model in reproducing the scattering parameters and some of the phase shifts is also not completely satisfactory. The zero (relative) energy scattering parameters predicted by the Hannover  $\Delta\Delta$  model are collected in Table III. The slight discrepancy in the  ${}^3S_1$  parameters is partly due to the fact that in this channel the renormalization energy  $E_r$  was chosen to reproduce the deuteron binding rather than the zero (relative) energy parameters. The rather large discrepancy in the  ${}^1S_0$  scattering length and effective range is, however, largely due to the failure of the chosen renormalization procedure to adequately reproduce the Paris potential at the renormalization energy, as discussed above. The phase shifts calculated from the Hannover  $\Delta\Delta$  model differ most from the Paris values in the  ${}^1S_0$  and  ${}^3S_1$  partial waves. It is found that the Hannover  $\Delta\Delta$ -model  ${}^1S_0$  phase shift deviates increasingly from the Paris phase shift as the energy increases above threshold, being larger than the Paris value by about  $14^\circ$  at  $E_{\text{lab}} = 100$  MeV, while the corresponding difference for the  ${}^3S_1$  phase shift is about  $3.3^\circ$  at  $E_{\text{lab}} = 100$  MeV. All the other Hannover  $\Delta\Delta$ -model phase shifts differ from the corresponding Paris values by less than  $1^\circ$  from threshold to  $E_{\text{lab}} = 100$  MeV.

The poor performance of the Hannover  $\Delta\Delta$  model in reproducing the  ${}^1S_0$  scattering parameters is a potentially serious defect. Just how serious a defect, however, depends on its root source. To the extent that the Hannover model's handling of the  $\Delta$  sectors is reliable, the poor two-body  ${}^1S_0$  scattering parameters need to be repaired by modifications to the  $NN$   ${}^1S_0$  potential. This would require substantially reducing the attraction of the potential, in order to both reduce the scattering length and increase the effective range, and thereby recover the correct  ${}^1S_0$  parameter values. Using the scale of Ref. [7] for the effective range, and the scale of Ref. [8] for the scattering length, these modifications to the  $NN$  potential could entail a reduction of the triton binding energy by about 900 keV. In this case, the Hannover  $\Delta\Delta$  model is unreliable in that it omits any such modifications.

However, the majority of the  $\Delta\Delta$  model's  ${}^1S_0$  defect (beyond its  $N\Delta$  component already described in Ref. [1]) is attributable to the inadequacy of the approximate renormalization procedure for this channel. This part of the defect requires corrections to the treatment of  $\Delta$

effects, rather than to the  $NN$  sector potential. In this case, the  $\Delta\Delta$  model's poor two-body  ${}^1S_0$  predictions must be regarded as partly spurious, representative not of the basic  $\Delta$  couplings of the model but of an inadequate renormalization. Consequently, the predicted effect of the  $\Delta$  couplings of the  ${}^1S_0$  channel on the triton binding energy (beyond that of the one- $\Delta$  model), which (as in the one- $\Delta$  model) is almost entirely the two-body dispersive effect, is what is not reliable. As will be seen in Sec. IV, the  ${}^1S_0$  dispersive contribution to the triton binding energy from the added sophistications of the  $\Delta\Delta$  model (beyond the one- $\Delta$  model) is only about 140 keV. This contribution is small, both relative to the corresponding one- $\Delta$  effect of Ref. [1] ( $\sim 450$  keV) and relative to the scale of other effects which arise in the study of the three-body implications of the Hannover  $\Delta\Delta$  model. Thus although an improved treatment of the  ${}^1S_0$  channel would no doubt modify the predicted 140 keV repulsive contribution, this is of secondary importance to this investigation. In other words, the large  $\Delta$ -induced changes in the  ${}^1S_0$  parameters in the Hannover  $\Delta\Delta$  model are correlated with only a small decrease in the triton binding (just the opposite of the large increase in the binding that would be expected from  $NN$ -only calculations). Thus the correction to  $E_T$  from an improved treatment of the  ${}^1S_0$  channel may be a very minor one. Of course, the  ${}^1S_0$  defect associated with the  $N\Delta$  channels [1] has to be kept in mind as well, especially to the extent that its compensation in more sophisticated models introduces modifications to the  $NN$ -sector potential.

With these caveats, based on the foregoing considerations, and for the following three additional reasons, the three-body implications of the Hannover  $\Delta\Delta$  model continue to be of interest: (1) Subsequent three-body investigations will use the more complicated Argonne V-28 potential [4] which is free of shortcomings relative to fitting the two-body  $NN$  data, so that such defects can be eliminated in this context; (2) the qualitative three-body implications of the Hannover  $\Delta\Delta$  model are of great schematic importance, viz., the overview of trinuclear  $\Delta$  effects depicted by the perturbative analysis of Ref. [3], and summarized in the Introduction to this paper; and (3) the most important discoveries of this paper include the principal aspects of a crucial doorway mechanism for  $\Delta\Delta$ -induced three-body force effects, the appreciable size of  $\Delta\Delta$ -induced three-body force effects, and large-scale cancellations between different  $N\Delta$  and  $\Delta\Delta$  contributions to the triton binding—all of which primarily involve channels other than the  ${}^1S_0$  channel.

#### IV. RESULTS

The calculations relevant to the  $\Delta\Delta$  investigations of this paper fall broadly into four categories: (1) Standard nucleons-only calculations based on the Paris  $NN$  potential, denoted "Paris"; (2) the HB1\* calculations of Ref. [1] which use the Hannover A1 one- $\Delta$  force model in the two-body system, with the three-body channels being those channels (with at most one  $\Delta$ ) built from the employed two-body channels, except as otherwise restricted. However, when the spectator particle is a  $\Delta$ , Paris  $NN$ -

TABLE III. Scattering length ( $a$ ) and effective range ( $r$ ) parameters predicted by the Hannover  $\Delta\Delta$  model, as compared to those predicted by the Paris potential.

Model	${}^1S_0$		${}^3S_1$	
	$a$ (fm)	$r$ (fm)	$a$ (fm)	$r$ (fm)
Hannover $\Delta\Delta$	-24.89	2.55	5.39	1.72
Paris	-17.55	2.86	5.43	1.77

$NN$  amplitudes are used in place of the A1 model  $NN$ - $NN$  amplitudes; (3) two types of dispersive calculations. “DISP1” calculations which use either the Hannover A1 force model or the Hannover  $\Delta\Delta$  force model in the two-body system, but allow only  $NNN$  channels (and hence use only the  $NN$ - $NN$  two-body amplitudes) in the solution of the Faddeev equation. “DISP2” calculations which mimic the three-body HB1\* calculations (no  $N\Delta\Delta$  channels are included) except that the Hannover  $\Delta\Delta$  force model is used in the two-body system irrespective of the type of spectator particle. DISP1 calculations which use the A1 force model are just the dispersive calculations studied in Ref. [1]. They provide a baseline of comparison with which to infer the strength of one- $\Delta$ -induced 3BF effects from the results of full one- $\Delta$ -model calculations. DISP1 calculations which use the Hannover  $\Delta\Delta$  model include all of the dispersive effects of the  $\Delta\Delta$  model on the  $NN$ - $NN$  amplitudes. Comparison of the two types of DISP1 results isolates an additional dispersive effect of the  $\Delta\Delta$  model. DISP2 calculations assess the net results of all contributions to the triton binding except for the effect of allowing  $N\Delta\Delta$  channels in the Faddeev calculation. They therefore expose the added dispersive effect which the  $\Delta\Delta$  model two-body interaction produces in the one- $\Delta$  three-body calculations, as well as provide a baseline for isolating the 3BF effects which arise from  $\Delta\Delta$  channels; and, finally, (4) full “HDD” calculations which use the Hannover  $\Delta\Delta$  force model in the two-body system, with the three-body channels being those (with at most two  $\Delta$ 's) built from the employed two-body channels, except as otherwise restricted.

Because the  $\Delta\Delta$  model is built on the one- $\Delta$  model, the subsequent discussion is mostly framed from the perspective of attributing effects to one model or the other. Basically, (1) the difference between A1 model DISP1 and Paris results yields the dispersive effect of the one- $\Delta$  model, (2) the difference between the HB1\* result and the A1 DISP1 result gives the three-body-force effect (3BFE) of the one- $\Delta$  model, (3) the difference between the DISP2 and HB1\* results gives the additional dispersive effect of the  $\Delta\Delta$  model, and (4) the difference between HDD and DISP2 results gives the  $\Delta\Delta$  3BFE. However, a slightly different perspective is also relevant. This perspective focuses entirely on the  $\Delta\Delta$  model itself and attributes binding energy effects accordingly. Basically, (1) the difference between  $\Delta\Delta$  model DISP1 and Paris results yields the  $\Delta\Delta$ -model dispersive effect (and comparison of this with the one- $\Delta$  model dispersive effect yields an additional  $\Delta\Delta$  model dispersive effect), (2) the difference between DISP2 and  $\Delta\Delta$  model DISP1 results yields the one- $\Delta$  3BFE of the  $\Delta\Delta$  model, and (3) the difference between the HDD and DISP2 results yields the  $\Delta\Delta$  3BFE as before. The two perspectives differ in their attribution of the three-body effects caused by the changes in the two-body amplitudes involving  $N\Delta$  channels which are induced by the additional  $\Delta\Delta$ -model interactions. In the first case these effects increase the dispersive effect of the  $\Delta\Delta$  model, whereas in the second they instead reduce the one- $\Delta$  3BFE of the  $\Delta\Delta$  model by a like amount, the end result for  $E_T$  being the same. This should be kept in mind in subsequent discussions involving the  $\Delta\Delta$  disper-

sive effect and the one- $\Delta$  3BFE.

In the following discussion, it is useful to have available a notation which explicitly distinguishes the pair and spectator particles which make up a given three-body channel. To this end, the convention is adopted that parentheses are used to specify the pair. For example, an  $NN\Delta$  channel with an  $N\Delta$  pair is denoted as  $N(N\Delta)$  while one with a  $\Delta$  spectator is denoted as  $\Delta(NN)$ .

The major results reported in this work follow primarily from two- and three-body calculations which restrict the total and orbital angular momentum of the pair to be  $J \leq 2$  and  $L(N\Delta), L(\Delta\Delta) \leq 2$ , respectively. The truncation of channels with  $J \geq 3$  and  $L(N\Delta), L(\Delta\Delta) \geq 3$  represents a considerable reduction in the size and complexity of the calculations. Therefore, the remainder of this section is broken into two subsections: Section IV A is concerned with detailing the justification for these truncations, and with estimating the size of the corrections to the binding energy which can be expected to come from the truncated channels; Section IV B presents the results obtained from the restricted calculations and the net results which then follow from the applicable corrections. Section IV A can be skipped by those not interested in the ancillary details.

#### A. Truncations and corrections

The one- $\Delta$  studies of Ref. [1] form a natural basis for the  $\Delta\Delta$  investigations reported in this paper. In Ref. [1] it was found that  $NNN$  and  $NN\Delta$  channels with  $J=3,4$  make only a small contribution to the triton binding energy,  $E_T$  (see Table XII of Ref. [1]). For purely  $NNN$  calculations this is a well-known result. For the  $NN\Delta$  channels the  $N$ - $\Delta$  mass difference pushes the channels further off-shell causing an additional suppression (beyond that of the  $NNN$  channels) of channels with larger  $L$ . Thus for three-body calculations restricted to the  $NNN$  and  $NN\Delta$  sectors, channels with  $J \geq 5$  can be safely neglected. For  $N\Delta\Delta$  channels the off-shell effect is only enhanced by the presence of two  $\Delta$ 's, so that in this case it is also expected that  $J \geq 5$  can be safely ignored. Further support for this expectation will be evident in the trends found for the  $\Delta\Delta$  contributions for  $J \leq 4$ . Thus these  $\Delta\Delta$  studies begin by adopting the restriction  $J \leq 4$ .

To justify treating the  $J=3,4$   $NN\Delta$  and  $N\Delta\Delta$  channels as a correction, it is necessary to recall several conclusions from the one- $\Delta$  studies of Ref. [1]. First, the net contribution of  $J=3,4$  channels was largely independent of which  $J \leq 2$  channels were included, so that this contribution could be simply added by hand to the results of  $J \leq 2$  calculations. Due to the dominance of the  $J \leq 2$   $NNN$  channels, this is not expected to be changed by the inclusion of  $N\Delta\Delta$  states, and the final estimated result for the Hannover  $\Delta\Delta$  model with  $J \leq 4$  will be obtained by adding a correction for the truncated  $J \geq 3$  channels,  $\Delta E_T(J=3,4)$ , to the  $J \leq 2$  results. Second, Ref. [1] found that the contribution of  $NNN$   $J=3,4$  channels in  $NNN + NN\Delta$  calculations was  $\sim 90$  keV, about 10 keV more attractive than the corresponding contribution in the purely Paris  $NNN$  calculation. This 10 keV increase

is attributable to the combination of a 10 keV ( $N\Delta$ ) repulsive dispersive effect and 20 keV of attraction due to  $NN\Delta$  coupling. The next relevant result from Ref. [1] is that the contributions to  $E_T$  from those  $J=3,4$   $NN\Delta$  channels either with  $L(N\Delta) \geq 3$  or with a  $\Delta$  spectator were completely negligible. Because of the enhanced off-shell effect of the  $N$ - $\Delta$  mass difference, the corresponding truncation of  $N(\Delta\Delta)$  channels with  $L(\Delta\Delta) \geq 3$  is expected to be at least as well motivated. As will be discussed more fully in the following subsection, the same cannot be assumed for channels with a  $\Delta$  spectator and an  $N\Delta$  pair, nor can the  $J=3,4$  ( $NN$ ) $\Delta$  channels be assumed to be entirely negligible. The contribution from these three-body channels will be, however, included in the estimated 3BF contribution from all  $N\Delta\Delta$   $J=3,4$  channels. Finally, Ref. [1] showed that the  $N(N\Delta)$   $J=3,4$  channels' contribution is at  $\sim 50$  keV, about an order of magnitude smaller than the corresponding  $J=2$  contribution. Approximately this same ratio is observed for the  $N\Delta$  dispersive effect as well. As is seen shortly, the inclusion of  $\Delta\Delta$  channels adds about 10 keV to the dispersive effect seen in the  $J=3,4$   $NNN$  channels' contribution to  $E_T$ , and this is again about an order of magnitude smaller than the corresponding  $J=2$  dispersive effect. Thus  $J=3,4$   $\Delta$  effects scale rather consistently at about  $\frac{1}{10}$  of the corresponding  $J=2$  effects. Based on this observation, it is assumed in this work that the 3BF contribution from  $J=3,4$   $N\Delta\Delta$  channels can be approximately taken into account via a correction equal to  $\frac{1}{10}$  of the  $J=2$   $N\Delta\Delta$  3BF contribution. Because the attractive 3BF effect of  $J=2$   $N\Delta\Delta$  channels is much smaller than the corresponding  $NN\Delta$  contribution, this yields a very minor correction and it should not be an unreasonable approximation. Similarly, the added repulsive three-body effect induced by the  $\Delta\Delta$  model through the changes made in the two-body amplitudes involving  $N\Delta$  channels (e.g., the difference between the one- $\Delta$  3BF effect seen in the one- $\Delta$  model and that of the  $\Delta\Delta$  model itself) is also taken to scale by  $\sim \frac{1}{10}$  in going from  $J=2$  to  $J=3,4$ . The net result of all of this is that the estimated net correction for  $J=3,4$   $\Delta\Delta$  effects is given by  $\frac{1}{10}$  of the  $J=2$  effect, i.e., by  $\frac{1}{10}$  of the  $J=2$  contribution to the difference between  $J \leq 2$  HDD and HB1\* results for  $E_T$ . Ultimately this correction is found to be negligible because  $J=2$   $\Delta\Delta$  dispersive and 3BF effects cancel almost exactly, leaving only a very small net  $J=2$   $\Delta\Delta$  effect. In summation, the correction for the truncated three-body channels with  $J=3,4$  is the sum of the 90 keV  $NNN$  channels' contribution, the 50 keV from the  $N(N\Delta)$  channels with  $L(N\Delta) \leq 2$ , and the estimated  $J=3,4$   $\Delta\Delta$  effect. Thus, in this work, the net effect on  $E_T$  from  $J=3,4$  channels is taken to be an increased binding of

$$\Delta E_T(J=3,4) \approx 140 \text{ keV} + \frac{1}{10} [\Delta\Delta(J=2 \text{ effect})], \quad (22)$$

which is to be added by hand to the results for  $J \leq 2$ . Consequently, except for an examination of  $\Delta\Delta$  dispersive effects on  $J \leq 4$   $NNN$  calculations, the actual  $\Delta\Delta$  calculations are restricted to  $J \leq 2$ .

The scope of the main three-body problem is reduced still further through the truncation of those  $J \leq 2$  chan-

TABLE IV. The  $J \leq 2$  two-body channels with  $L(N\Delta)$ ,  $L(\Delta\Delta) \leq 2$ .

No.	$J$	$T$	$L$	$S$	$N$	$N_z$
1	0	1	0	0	1	-1
2	0	1	2	2	1	0
3	0	1	0	0	1	1
4	0	1	2	2	1	1
5	0	1	1	1	1	-1
6	0	1	1	1	1	0
7	0	1	1	1	1	1
8	1	0	0	1	1	-1
9	1	0	2	1	1	-1
10	1	0	0	1	1	1
11	1	0	2	1	1	1
12	1	0	2	3	1	1
13	1	0	1	0	1	-1
14	1	0	1	0	1	1
15	1	0	1	2	1	1
16	1	1	1	1	1	-1
17	1	1	1	1	1	0
18	1	1	1	1	1	1
19	1	1	1	2	0	0
20	2	0	2	1	1	-1
21	2	0	2	1	1	1
22	2	0	2	3	1	1
23	2	1	2	0	1	-1
24	2	1	0	2	1	0
25	2	1	2	2	1	0
26	2	1	2	0	1	1
27	2	1	0	2	1	1
28	2	1	2	2	1	1
29	2	1	2	1	0	0
30	2	1	1	1	1	-1
31	2	1	3	1	1	-1
32	2	1	1	1	1	0
33	2	1	1	1	1	1
34	2	1	1	3	1	1
35	2	1	1	2	0	0

nels with  $L(N\Delta)$ ,  $L(\Delta\Delta)=3,4$ . The justification for this truncation again relies partly on results of Ref. [1]. For the Hannover one- $\Delta$  model the net contribution of  $J \leq 2$  and  $L(N\Delta)=3,4$  channels was small ( $\sim 60$  keV of repulsion), and was, to a large extent, already in place at the

TABLE V. The  $J \leq 2$  two-body channels with  $L(N\Delta)$ ,  $L(\Delta\Delta)=3,4$ .

No.	$J$	$T$	$L$	$S$	$N$	$N_z$
1	0	1	3	3	1	1
2	1	0	4	3	1	1
3	1	0	3	2	1	1
4	1	1	3	3	1	1
5	1	1	3	2	0	0
6	2	0	4	3	1	1
7	2	1	4	2	1	0
8	2	1	4	2	1	1
9	2	1	3	1	1	0
10	2	1	3	1	1	1
11	2	1	3	3	1	1
12	2	1	3	2	0	0

TABLE VI. The additional  $NN$  channels with  $J=3,4$ .

No.	$J$	$T$	$L$	$S$	$N$	$N_z$
1	3	0	2	1	1	-1
2	3	0	4	1	1	-1
3	3	0	3	0	1	-1
4	3	1	3	1	1	-1
5	4	0	4	1	1	-1
6	4	1	4	0	1	-1
7	4	1	3	1	1	-1
8	4	1	5	1	1	-1

$J \leq 1$  level, with only  $\sim 20$  keV attributable to  $J=2$   $NN\Delta$  channels. Further, it can be inferred from the results of Ref. [1] that this 20 keV is largely due to dispersive effects, implying that the  $J=2, L(N\Delta)=3,4$  one- $\Delta$ -model 3BF effect is negligible (see Table XII of Ref. [1] and the accompanying discussion). Consistent with this, the  $J=2, L(\Delta\Delta)=3,4$   $\Delta\Delta$  3BF contribution is also assumed to be negligible. A series of preliminary calculations, to be discussed shortly, shows that the corresponding dispersive effect is also negligible. All that remains is the  $J \leq 1, L(N\Delta), L(\Delta\Delta)=3,4$  contribution, which has been calculated for the full Hannover  $\Delta\Delta$  model and is found

TABLE VII. The  $J \leq 1$  three-body channels with  $L(N\Delta), L(\Delta\Delta) \leq 2$ .

No.	$J$	$T$	$L$	$S$	$N$	$N_z$	$l$	$j$	$n_z$
1	0	1	0	0	1	-1	0	1/2	-1/2
2	0	1	0	0	1	-1	2	1/2	1/2
3	0	1	2	2	1	0	0	1/2	-1/2
4	0	1	2	2	1	0	2	1/2	1/2
5	0	1	0	0	1	1	0	1/2	-1/2
6	0	1	2	2	1	1	0	1/2	-1/2
7	0	1	1	1	1	-1	1	1/2	-1/2
8	0	1	1	1	1	-1	1	1/2	1/2
9	0	1	1	1	1	0	1	1/2	-1/2
10	0	1	1	1	1	0	1	1/2	1/2
11	0	1	1	1	1	1	1	1/2	-1/2
12	1	0	0	1	1	-1	0	1/2	-1/2
13	1	0	0	1	1	-1	2	3/2	-1/2
14	1	0	2	1	1	-1	0	1/2	-1/2
15	1	0	2	1	1	-1	2	3/2	-1/2
16	1	0	0	1	1	1	0	1/2	-1/2
17	1	0	0	1	1	1	2	3/2	-1/2
18	1	0	2	1	1	1	0	1/2	-1/2
19	1	0	2	1	1	1	2	3/2	-1/2
20	1	0	2	3	1	1	0	1/2	-1/2
21	1	0	2	3	1	1	2	3/2	-1/2
22	1	0	1	0	1	-1	1	1/2	-1/2
23	1	0	1	0	1	-1	1	3/2	-1/2
24	1	0	1	0	1	1	1	1/2	-1/2
25	1	0	1	0	1	1	1	3/2	-1/2
26	1	0	1	2	1	1	1	1/2	-1/2
27	1	0	1	2	1	1	1	3/2	-1/2
28	1	1	1	1	1	-1	1	1/2	-1/2
29	1	1	1	1	1	-1	1	3/2	-1/2
30	1	1	1	1	1	-1	1	1/2	1/2
31	1	1	1	1	1	-1	1	3/2	1/2
32	1	1	1	1	1	-1	3	3/2	1/2
33	1	1	1	1	1	0	1	1/2	-1/2
34	1	1	1	1	1	0	1	3/2	-1/2
35	1	1	1	1	1	0	1	1/2	1/2
36	1	1	1	1	1	0	1	3/2	1/2
37	1	1	1	1	1	0	3	3/2	1/2
38	1	1	1	1	1	1	1	1/2	-1/2
39	1	1	1	1	1	1	1	3/2	-1/2
40	1	1	1	2	0	0	1	1/2	-1/2
41	1	1	1	2	0	0	1	3/2	-1/2
42	1	1	1	2	0	0	1	1/2	1/2
43	1	1	1	2	0	0	1	3/2	1/2
44	1	1	1	2	0	0	3	3/2	1/2



to be a small, repulsive effect of  $\sim 10$  keV. Because this calculated value includes all of the one- $\Delta$  as well as the  $\Delta\Delta$  contributions, the applicable correction for eliminating the  $L(N\Delta)$ ,  $L(\Delta\Delta)=3,4$  channels with  $J \leq 2$  from explicit consideration is just the sum of the 20 keV repulsive effect from the  $J=2$   $NN\Delta$  channels and the calculated contribution in the  $J \leq 1$  case (i.e., 10 keV). Thus, the net correction is just a 30 keV repulsion. Combining this correction with  $\Delta E_T(J=3,4)$  yields the net correction to the  $J \leq 2$ ,  $L(N\Delta) \leq 2$ ,  $L(\Delta\Delta) \leq 2$  calculations due to channels with  $J=3,4$  or  $L(N\Delta)$ ,  $L(\Delta\Delta)=3,4$ :

$$\Delta E_T(3,4) \approx 110 \text{ keV} + \frac{1}{10} [\Delta\Delta(J=2 \text{ effect})] . \quad (23)$$

Based on this discussion, and with further support from  $J \leq 2$  calculations presented later, the main ( $J \leq 2$ ) three-body problem can thus be restricted to  $L(N\Delta)$ ,  $L(\Delta\Delta) \leq 2$  as well.

With the effective scope of the ( $NNN + NN\Delta + N\Delta\Delta$ ) system reduced to  $J \leq 2$ , and  $L(N\Delta)$ ,  $L(\Delta\Delta) \leq 2$ , the resultant three-body problem is still quite formidable. In

fact, it involves 35 two-body channels and 108 three-body channels. The 35 two-body channels yield a total of 169 two-body amplitudes. Although solving this problem is within our present capabilities, we have refrained from doing so for reasons of economy. Instead, a well-motivated net result for  $E_T$  is constructed by combining the results of several smaller calculations. This constructive approach also has the advantage of exposing both some important physical mechanisms and the interplay between various contributions.

For convenience, the two- and three-body channels relevant to this work are collected in Tables IV–XI. Tables IV–VI hold the two-body channels, while Tables VII–XI hold the three-body channels. Table IV lists the 35 two-body channels with  $J \leq 2$  and  $L(N\Delta)$ ,  $L(\Delta\Delta) \leq 2$ , Table V lists the additional 12  $N\Delta$  and  $\Delta\Delta$   $J \leq 2$  two-body channels with  $L(N\Delta)$ ,  $L(\Delta\Delta)=3,4$ , and Table VI lists the additional 8  $NN$  channels with  $J=3,4$  which are relevant to the dispersive calculations. Tables VII–IX contain the 108 three-body channels with  $J \leq 2$  and  $L(N\Delta)$ ,  $L(\Delta\Delta) \leq 2$ . Table VII contains the 44  $J \leq 1$

TABLE VIII. The  $J^\pi=2^+$  three-body channels with  $L(N\Delta)$ ,  $L(\Delta\Delta) \leq 2$ .

No.	$J$	$T$	$L$	$S$	$N$	$N_z$	$l$	$j$	$n_z$
1	2	0	2	1	1	-1	2	3/2	-1/2
2	2	0	2	1	1	-1	2	5/2	-1/2
3	2	0	2	1	1	1	2	3/2	-1/2
4	2	0	2	1	1	1	2	5/2	-1/2
5	2	0	2	3	1	1	2	3/2	-1/2
6	2	0	2	3	1	1	2	5/2	-1/2
7	2	1	2	0	1	-1	2	3/2	-1/2
8	2	1	2	0	1	-1	2	5/2	-1/2
9	2	1	2	0	1	-1	0	3/2	1/2
10	2	1	2	0	1	-1	2	3/2	1/2
11	2	1	2	0	1	-1	2	5/2	1/2
12	2	1	2	0	1	-1	4	5/2	1/2
13	2	1	0	2	1	0	2	3/2	-1/2
14	2	1	0	2	1	0	2	5/2	-1/2
15	2	1	0	2	1	0	0	3/2	1/2
16	2	1	0	2	1	0	2	3/2	1/2
17	2	1	0	2	1	0	2	5/2	1/2
18	2	1	0	2	1	0	4	5/2	1/2
19	2	1	2	2	1	0	2	3/2	-1/2
20	2	1	2	2	1	0	2	5/2	-1/2
21	2	1	2	2	1	0	0	3/2	1/2
22	2	1	2	2	1	0	2	3/2	1/2
23	2	1	2	2	1	0	2	5/2	1/2
24	2	1	2	2	1	0	4	5/2	1/2
25	2	1	2	0	1	1	2	3/2	-1/2
26	2	1	2	0	1	1	2	5/2	-1/2
27	2	1	0	2	1	1	2	3/2	-1/2
28	2	1	0	2	1	1	2	5/2	-1/2
29	2	1	2	2	1	1	2	3/2	-1/2
30	2	1	2	2	1	1	2	5/2	-1/2
31	2	1	2	1	0	0	2	3/2	-1/2
32	2	1	2	1	0	0	2	5/2	-1/2
33	2	1	2	1	0	0	0	3/2	1/2
34	2	1	2	1	0	0	2	3/2	1/2
35	2	1	2	1	0	0	2	5/2	1/2
36	2	1	2	1	0	0	4	5/2	1/2

TABLE IX. The  $J^\pi=2^-$  three-body channels with  $L(N\Delta), L(\Delta\Delta)\leq 2$ .

No.	$J$	$T$	$L$	$S$	$N$	$N_z$	$l$	$j$	$n_z$
1	2	1	1	1	1	-1	1	3/2	-1/2
2	2	1	1	1	1	-1	3	5/2	-1/2
3	2	1	1	1	1	-1	1	3/2	1/2
4	2	1	1	1	1	-1	3	3/2	1/2
5	2	1	1	1	1	-1	1	5/2	1/2
6	2	1	1	1	1	-1	3	5/2	1/2
7	2	1	3	1	1	-1	1	3/2	-1/2
8	2	1	3	1	1	-1	3	5/2	-1/2
9	2	1	3	1	1	-1	1	3/2	1/2
10	2	1	3	1	1	-1	3	3/2	1/2
11	2	1	3	1	1	-1	1	5/2	1/2
12	2	1	3	1	1	-1	3	5/2	1/2
13	2	1	1	1	1	0	1	3/2	-1/2
14	2	1	1	1	1	0	3	5/2	-1/2
15	2	1	1	1	1	0	1	3/2	1/2
16	2	1	1	1	1	0	3	3/2	1/2
17	2	1	1	1	1	0	1	5/2	1/2
18	2	1	1	1	1	0	3	5/2	1/2
19	2	1	1	1	1	1	1	3/2	-1/2
20	2	1	1	1	1	1	3	5/2	-1/2
21	2	1	1	3	1	1	1	3/2	-1/2
22	2	1	1	3	1	1	3	5/2	-1/2
23	2	1	1	2	0	0	1	3/2	-1/2
24	2	1	1	2	0	0	3	5/2	-1/2
25	2	1	1	2	0	0	1	3/2	1/2
26	2	1	1	2	0	0	3	3/2	1/2
27	2	1	1	2	0	0	1	5/2	1/2
28	2	1	1	2	0	0	3	5/2	1/2

channels, Table VIII the 36  $J^\pi=2^+$  channels, and Table IX the 28  $J^\pi=2^-$  channels. This grouping of the 108 three-body channels of the main three-body problem of this work corresponds to the pattern used in its investigation. Table X holds the 12 additional three-body channels with  $J\leq 1$  and  $L(N\Delta), L(\Delta\Delta)=3,4$  needed for the corresponding calculation referred to above. Similarly, Table XI holds the additional 16  $J=3,4$   $NNN$  channels relevant to the dispersive calculations.

Results from dispersive calculations of type DISP1 are displayed in Tables XII and XIII. The results in Table XII are for  $L(N\Delta), L(\Delta\Delta)\leq 2$  while those in Table XIII also include  $L(N\Delta), L(\Delta\Delta)=3,4$ . These tables show

TABLE X. The  $J\leq 1$  three-body channels with  $L(N\Delta), L(\Delta\Delta)=3,4$ .

No.	$J$	$T$	$L$	$S$	$N$	$N_z$	$l$	$j$	$n_z$
1	0	1	3	3	1	1	1	1/2	-1/2
2	1	0	4	3	1	1	0	1/2	-1/2
3	1	0	4	3	1	1	2	3/2	-1/2
4	1	0	3	2	1	1	1	1/2	-1/2
5	1	0	3	2	1	1	1	3/2	-1/2
6	1	1	3	3	1	1	1	1/2	-1/2
7	1	1	3	3	1	1	1	3/2	-1/2
8	1	1	3	2	0	0	1	1/2	-1/2
9	1	1	3	2	0	0	1	3/2	-1/2
10	1	1	3	2	0	0	1	1/2	1/2
11	1	1	3	2	0	0	1	3/2	1/2
12	1	1	3	2	0	0	3	3/2	1/2

predicted triton binding energies and dispersive binding energy shifts (DISP) for the Hannover A1 one- $\Delta$  model ( $\Delta$ ) and for the Hannover  $\Delta\Delta$  model ( $\Delta\Delta$ ). The additional dispersive effect found for the  $\Delta\Delta$  model (relative to the  $\Delta$  model) is isolated in the last column of the tables; the reader is reminded that the last three columns include the effect of the diagonal  $N\Delta$ - $N\Delta$  potential,  $V_{0,0}$ , as well as the effect of two  $\Delta$ 's. The additional  $\Delta\Delta$  dispersive effect is repulsive and large; at about 600 keV it is slightly

TABLE XI. The additional  $NNN$  channels for  $J=3,4$ .

No.	$J$	$T$	$L$	$S$	$N$	$N_z$	$l$	$j$	$n_z$
1	3	0	2	1	1	-1	2	5/2	-1/2
2	3	0	2	1	1	-1	4	7/2	-1/2
3	3	0	4	1	1	-1	2	5/2	-1/2
4	3	0	4	1	1	-1	4	7/2	-1/2
5	3	0	3	0	1	-1	3	5/2	-1/2
6	3	0	3	0	1	-1	3	7/2	-1/2
7	3	1	3	1	1	-1	3	5/2	-1/2
8	3	1	3	1	1	-1	3	7/2	-1/2
9	4	0	4	1	1	-1	4	7/2	-1/2
10	4	0	4	1	1	-1	4	9/2	-1/2
11	4	1	4	0	1	-1	4	7/2	-1/2
12	4	1	4	0	1	-1	4	9/2	-1/2
13	4	1	3	1	1	-1	3	7/2	-1/2
14	4	1	3	1	1	-1	5	9/2	-1/2
15	4	1	5	1	1	-1	3	7/2	-1/2
16	4	1	5	1	1	-1	5	9/2	-1/2

TABLE XII. DISP1  $\Delta$  and  $\Delta\Delta$  results for the triton binding energy (in MeV) with  $L(N\Delta)$ ,  $L(\Delta\Delta)\leq 2$ . Net dispersive effects (in keV) for each model (relative to the Paris result) are presented in the respective columns headed DISP. The corresponding Paris results (in MeV) are shown for completeness. The last column, labeled DIFF, shows the added dispersive effect (in keV) of the  $\Delta\Delta$  model. The special results of the last row, denoted by an asterisk, exclude  $\Delta\Delta$  channels from the determination of the  $J=1$   $NN$  amplitudes used in the Faddeev calculations.

Channels	Paris	DISP1 ( $\Delta$ )	DISP ( $\Delta$ )	DISP1 $\Delta\Delta$	DISP $\Delta\Delta$	DIFF
$J\leq 4, \pi=\pm$	7.46(34)	6.90	560	6.29	1170	610
$J\leq 2, \pi=\pm$	7.38(18)	6.83	550	6.23	1150	600
$J\leq 2, \pi=+$	7.41( 9)	6.93	480	6.34	1070	590
$J\leq 1, \pi=\pm$	7.10(10)	6.64	460	6.12	980	520
$J\leq 1, \pi=+$	7.30( 5)	6.85	450	6.28	1020	570
$J\leq 1, \pi=+, *$	7.30( 5)	6.85	450	6.71	590	140

larger, in fact, than the corresponding DISP( $\Delta$ ) effect.

A number of other results can also be inferred from the dispersive calculations of Tables XII and XIII, including some of the results already employed in circumscribing the scope of the main three-body problem, in obtaining channel-truncation corrections, and in assessing the credibility of the Hannover  $\Delta\Delta$  model at the end of Sec. III. First, comparing the first two rows of either table shows that the  $J=3,4$  channels contribute 20 keV of repulsion, with 10 keV coming from the one- $\Delta$  model and an additional 10 keV from the extensions to the one- $\Delta$  model which form the  $\Delta\Delta$  model. Both of these dispersive contributions are included as part of the net  $J=3,4$  correction, and both are seen from the tables to be about an order of magnitude smaller than the corresponding  $J=2$  contribution, as indicated in the second paragraph of this subsection. Next, comparing columns six between Tables XII and XIII, one sees that the total contribution of the  $L(N\Delta)$ ,  $L(\Delta\Delta)=3,4$  channels to the total ( $\Delta+\Delta\Delta$ ) dispersive effect is a 50 keV increase of the effect. One notes, furthermore, that this total contribution is already in place at the  $J\leq 2$  level, so that the  $L(N\Delta)$ ,  $L(\Delta\Delta)=3,4$  dispersive effect from the  $J=3,4$  channels is entirely negligible. Of the 50 keV increase, a comparison of the fourth columns of the two tables shows that 40 keV can be attributed to the original Hannover one- $\Delta$  model. One sees from the seventh columns that the additional 10 keV attributed to the Hannover  $\Delta\Delta$  model (beyond the  $\Delta$  contribution) is already fully accounted for at the  $J\leq 1$  level. Thus any additional  $J=2$  dispersive contribution from the Hannover  $\Delta\Delta$  model from  $L(N\Delta)$ ,  $L(\Delta\Delta)=3,4$  channels is also entirely negligible. Of the

40 keV  $L(N\Delta)=3,4$  dispersive contribution from the Hannover one- $\Delta$  model, the contribution from  $J=2$  channels is about 30 keV, while that from  $J=1$  channels is 10 keV. This 40 keV figure forms part of the net contribution of  $L(N\Delta)=3,4$  channels to the full  $J\leq 2$  Hannover one- $\Delta$  results of Ref. [1], and this net contribution is well represented by  $J\leq 1$  one- $\Delta$  three-body calculations and the 20 keV repulsive  $J=2$  correction as described in the third paragraph of this subsection. Combining these observations, the net  $J\leq 2$  DISP1 contribution of  $L(N\Delta)$ ,  $L(\Delta\Delta)=3,4$  channels is to a good approximation subsumed by  $J^\pi\leq 1^\pm$   $\Delta\Delta$ -model three-body calculations and the 20 keV repulsive  $J=2$  correction, a result already used in obtaining  $\Delta E_T(3,4)$ .

Also shown in the last row of Table XII or XIII is the 450 keV dispersive effect of the  $^1S_0$  channel's one- $\Delta$  coupling and the much smaller 140 keV dispersive effect of its  $\Delta\Delta$  coupling, both of which figured importantly in the discussion at the end of Sec. III. Finally, one notes from Table XII or XIII that most of the DISP1 effect beyond that of the single- $\Delta$  model arises from the  $J^\pi=1^+$  channels, i.e., from the  $\Delta\Delta$  couplings to the  $NN$   $^3S_1$ - $^3D_1$  channels.

Triton binding energy results from dispersive calculations of type DISP2 are displayed in Table XIV, for  $L(N\Delta)$ ,  $L(\Delta\Delta)\leq 2$ . Table XIV also shows the corresponding HB1\* results of Ref. [1] and the added dispersive effect (DISP) which the  $\Delta\Delta$  model two-body interaction induces in these one- $\Delta$  three-body calculations. The main finding of Table XIV is that the full DISP effect is "only" 880 keV. This is considerably smaller than the corresponding 1.3 MeV perturbative estimate of Ref. [3].

TABLE XIII. DISP1  $\Delta$  and  $\Delta\Delta$  results for the triton binding energy with  $L(N\Delta)$ ,  $L(\Delta\Delta)\leq 4$ . Results are presented as in Table XII.

Channels	Paris	DISP1 ( $\Delta$ )	DISP ( $\Delta$ )	DISP1 $\Delta\Delta$	DISP $\Delta\Delta$	DIFF
$J\leq 4, \pi=\pm$	7.46(34)	6.86	600	6.24	1220	620
$J\leq 2, \pi=\pm$	7.38(18)	6.79	590	6.18	1200	610
$J\leq 2, \pi=+$	7.41( 9)	6.92	490	6.32	1090	600
$J\leq 1, \pi=\pm$	7.10(10)	6.63	470	6.10	1000	530
$J\leq 1, \pi=+$	7.30( 5)	6.85	450	6.27	1030	580
$J\leq 1, \pi=+, *$	7.30( 5)	6.85	450	6.71	590	140

TABLE XIV.  $L(N\Delta)$ ,  $L(\Delta\Delta) \leq 2$  DISP2 results for the triton binding energy. The HB1\* results are from Ref. [1]. The only  $\Delta$ -spectator channel included in the calculations is the one with the  $NN$  pair in the  $^1S_0$  state. The column labeled DISP gives the added dispersive effect which the  $\Delta\Delta$ -model two-body interaction produces in the one- $\Delta$  three-body calculation. DISP2 and HB1\* results are in MeV, DISP results are in keV, and the number of three-body channels is indicated parenthetically.

Channels	HB1*	DISP2	DISP
$J \leq 2, \pi = \pm$	7.82(33)	6.94(35)	880
$J \leq 2, \pi = +$	7.01(15)	6.36(17)	650
$J \leq 1, \pi = \pm$	7.16(17)	6.46(17)	700
$J \leq 1, \pi = +$	6.81( 7)	6.21( 7)	600

The bulk of the DISP effect arises from  $J \leq 1$ , although the  $J=2$  channels' contribution of about 180 keV is also substantial. The fact that the  $J=2$  contribution is appreciable indicates that these channels will ultimately play an important role in the  $\Delta\Delta$  model's implications for the triton binding. For the  $J^\pi \leq 2^\pm$  case, calculations with  $L(N\Delta)$ ,  $L(\Delta\Delta) \leq 4$  (not shown) yield 60 keV reductions of both the HB1\* and DISP2 results, leaving the 880 keV DISP result unchanged. This also implies that the net  $L(N\Delta)$ ,  $L(\Delta\Delta) = 3,4$  DISP2 contribution is just the 60 keV  $L(N\Delta) = 3,4$  contribution observed in the full  $J \leq 2$  HB1\* calculations of Ref. [1], which is well represented (to within  $\sim 20$  keV from  $J=2$   $NN\Delta$  channels) at the  $J \leq 1$  level. This observation provides further support for the method used here to treat the  $J \leq 2$  channels with  $L(N\Delta)$ ,  $L(\Delta\Delta) = 3,4$ .

This completes the description of the results of the preliminary investigations. The contributions which various types of  $N\Delta\Delta$  channels make to the triton binding are examined next. In the process of this examination it is found that the net contribution of  $L(N\Delta)$ ,  $L(\Delta\Delta) = 3,4$  channels with  $J \leq 1$  is just the 10 keV cited earlier; together with the 20 keV  $J=2$   $NN\Delta$  contribution, this yields the total  $L(N\Delta)$ ,  $L(\Delta\Delta) = 3,4$  correction for  $J \leq 2$  and is the final component used in obtaining  $\Delta E_T(3,4)$ .

### B. $\Delta\Delta$ three-body-force effect

In this subsection, the  $\Delta\Delta$  3BF effects (3BFE) are investigated. The  $\Delta\Delta$  3BF arises from inclusion of Faddeev

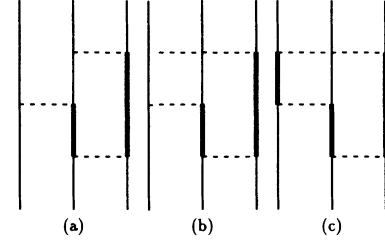


FIG. 3. The lowest-order three-body-force diagrams involving two  $\Delta$ 's (adjoint diagrams not shown).

amplitudes which have two  $\Delta$ 's, and their effects are isolated by subtracting DISP2 results from the full HDD results.  $\Delta\Delta$  3BF diagrams which can contribute in the Hannover  $\Delta\Delta$  model to lowest order are depicted in Fig. 3. The adjoints of the diagrams of Figs. 3(a) and 3(b) are not shown.

It turns out to be useful to frame the initial explorations in the context of the  $J^\pi \leq 1^\pm$  channels. Table XV compares full HDD results with the corresponding DISP2 results vs the  $\Delta$ -spectator channels included in the calculation. The inferred (attractive)  $\Delta\Delta$  3BFE is also indicated. All of the results shown are for  $J \leq 1$ , with  $L(N\Delta)$ ,  $L(\Delta\Delta) \leq 2$ . The reason for the preoccupation of Table XV with the  $\Delta$ -spectator channels will become evident shortly.

The first striking feature of Table XV is that there is no  $\Delta\Delta$  3BF contribution to the triton binding energy in a "standard" calculation in which only the  $^1S_0(NN)$   $\Delta$ -spectator channel is included, the second is the critical, seeming random dependence of the predicted  $\Delta\Delta$  3BFE on which  $\Delta$ -spectator channels are included in the calculation, and the third is the substantial  $\Delta\Delta$  3BF contribution found in the full  $J \leq 1$  calculation—much larger than that found in the original Hannover work [3]. All three of these features of the  $\Delta\Delta$  3BF contributions are, however, direct consequences of the structure of the Faddeev equation, Eq. (1).

The dominant sector of the three-body problem is the  $NNN$  sector. Consider Eq. (1), and the  $NNN$  sector  $\alpha'$  channels for the representative diagram of Fig. 3(a). The structure of Eq. (1) then generates  $(\Delta\Delta)N\alpha$  channels immediately from these  $NNN$  sector  $\alpha'$  channels. But then,

TABLE XV.  $J \leq 1$  HDD and DISP2 results (in MeV) for the triton binding energy versus the  $\Delta$ -spectator channels (chs) included in the calculation;  $L(N\Delta)$ ,  $L(\Delta\Delta) \leq 2$ . The last column gives the net  $\Delta\Delta$  three-body force effect exhibited by the corresponding HDD calculation (in keV). The number of three-body channels in the HDD calculations is indicated parenthetically.

$\Delta$ -spectator channels	HDD	DISP2	$\Delta\Delta$ 3BFE
$^1S_0(NN)\Delta$	6.46(32)	6.46	000
$^1S_0(NN)\Delta; ^5D_0(N\Delta)\Delta$	6.52(33)	6.46	60
All $J=0$ $(NN)\Delta$ and $(N\Delta)\Delta$	6.54(35)	6.46	80
$^1S_0(NN)\Delta; J=1$ $(N\Delta)\Delta$	6.51(38)	6.46	50
$^1S_0(NN)\Delta; \text{all } (N\Delta)\Delta$	6.56(40)	6.46	100
$^5D_0(N\Delta)\Delta; \text{all } (NN)\Delta$	6.42(37)	6.38	40
$^1S_0(NN)\Delta; \text{all } J=1$ chs	6.60(41)	6.38	220
All $(NN)\Delta$ and $(N\Delta)\Delta$ chs	6.67(44)	6.38	290

through what process do these  $(\Delta\Delta)N$  channels affect the important  $NNN$  sector? Consider in this regard Eq. (1), and the  $(\Delta\Delta)N$  sector  $\alpha'$  channels. Because of the geometrical coefficient which appears in Eq. (1), the  $\bar{\alpha}$  channels are necessarily  $(N\Delta)\Delta$ . If all  $(N\Delta)\Delta$  channels are excluded, then although  $\Delta\Delta$  Faddeev components are produced, they cannot couple back and affect the binding energy. This explains the first striking feature of Table XV, since  $(N\Delta)\Delta$  channels are clearly required for all of the diagrams of Fig. 3 (and their adjoints). The  $(N\Delta)\Delta$  channels serve as a doorway for  $\Delta\Delta$  3BF contributions. Note also that all of the  $\Delta\Delta$  3BF diagrams represented by Fig. 3 depend on two intermediate Faddeev amplitudes which contain one or two  $\Delta$ 's, and which are small relative to the dominant  $NNN$  amplitudes. For example, Fig. 3(a) depends on an intermediate  $\Delta\Delta N$  amplitude and an intermediate  $N\Delta$  amplitude. Stated differently, starting from the  $NNN$  sector Fig. 3(a) is generated by three "steps," i.e., three iterations of the Faddeev equation: the initial  $\alpha'$  channel is  $NNN$ , the  $\alpha'$  channel for the second iteration is  $(\Delta\Delta)N$ , and the  $\alpha'$  channel for the third is  $(NN)\Delta$ .

Because total angular momentum, total isospin, and parity are conserved by the two-body interaction, the second interaction in the diagrams represented by Figs. 3(a) and 3(b) can connect only  $(NN)\Delta$  channels and  $(N\Delta)\Delta$  channels which lie in the same  $(J^\pi, T)$  two-body sector. Thus to open the  $(N\Delta)\Delta$  doorway,  $(NN)\Delta$  channels of the same  $(J^\pi, T)$  are required in the calculation: only the diagram of Fig. 3(c) is an exception to this rule. This explains the second striking feature of Table XV: the sensitive dependence of the  $\Delta\Delta$  3BFE on just which  $\Delta$ -spectator channels are included in the calculations simply reflects the degree to which the doorway is opened by them. Keeping in mind the doorway mechanism, the relative importances of various contributions can now be read off from Table XV. For example: the fourth entry in this table, which allows only the  $^1S_0(NN)\Delta$  channel and those  $(N\Delta)\Delta$  channels with  $J=1$ , cannot have any contribution from the diagrams represented by Figs. 3(a) and 3(b) [due to the  $(J^\pi, T)$  rule—see Table VII in this regard]. Thus, the entire lowest-order contribution to the  $\Delta\Delta$ -induced 3BFE for this calculation ( $\sim 50$  keV) comes from the diagram of Fig. 3(c). As another example, one sees that only about 80 keV derives from the  $J=0$  channels, so that most ( $\sim 210$  keV) of the 290 keV  $\Delta\Delta$ -induced 3BFE for  $J \leq 1$  depends on the  $J=1$  channels. The difference in the DISP2 results of Table XV is largely just the repulsive effect observed in Ref. [1] to be associated with the  $J \leq 1$   $(NN)\Delta$  channels beyond the  $^1S_0(NN)\Delta$  channel.

From Table XV it is now evident that variations in the  $^1S_0(NN)$  channel can play only a very minor role in regard to  $\Delta\Delta$ -induced 3BF effects. As the last row of either Table XII or XIII shows, this channel plays a minor role in regard to  $\Delta\Delta$  dispersive effects, as well. These results figured importantly in assessing the merits of the Hannover  $\Delta\Delta$  force model in Sec. III.

The 290 keV  $\Delta\Delta$  3BFE contributed by the  $J \leq 1$  channels is by itself about three times the total  $\Delta\Delta$  3BFE observed in the perturbative calculations of Ref. [3]. The

third striking feature of Table XV is presumably explained by the fact that the limitations of the perturbative investigation of Ref. [3] left the  $\Delta\Delta$  3BF doorway largely closed.

The 56-channel,  $L(N\Delta), L(\Delta\Delta) \leq 4$ , analog of the full 44-channel result of Table XV was computed as well, and the result for the triton binding was found to be also about 6.67 MeV. The actual  $L(N\Delta), L(\Delta\Delta) = 3, 4$  contribution found in the 56-channel result is just under 10 keV, a result already used in determining  $\Delta E_T(3,4)$ . The importance of  $\Delta\Delta$ - $\Delta\Delta$  two-body amplitudes was also investigated, and these amplitudes were found to be entirely negligible. For example, analogs of the 35- and 41-channel results of Table XV in which the  $\Delta\Delta$ - $\Delta\Delta$  amplitudes are neglected differ from the corresponding results of Table XV by a repulsive effect of only 2–3 keV. Thus, the complexity of the remaining calculations is reduced by neglecting  $\Delta\Delta$ - $\Delta\Delta$  two-body amplitudes. The 44-channel  $J \leq 1$  system forms the core part of the final component of the determination of the implications of the Hannover  $\Delta\Delta$  model for the triton binding: assessing the  $\Delta\Delta$  3BF contribution from the  $J=2, L(N\Delta), L(\Delta\Delta) \leq 2$ , channels. Unlike the one- $\Delta$  investigations of Ref. [1], where most  $\Delta$ -spectator channels could be treated essentially as an afterthought, here the doorway mechanism demands that  $\Delta$ -spectator channels be treated as an integral part of the development. Thus the following investigation of the 3BF contributions of the  $J=2$  channels includes  $(NN)\Delta$  and  $(N\Delta)\Delta$  channels on an equal basis with the corresponding  $(N\Delta)N$  and  $(\Delta\Delta)N$  channels. The 44-channel calculation was also used to gauge  $\Delta$  components in the trinuclear wave function: the one- $\Delta$  probability was found to be 1.82%, and the  $\Delta\Delta$  probability 4.44%. The  $\Delta\Delta$  figure is comparable to that of Ref. [3], while the  $\Delta\Delta$  model's one- $\Delta$  component here is somewhat reduced from that of the one- $\Delta$  model, which is 2.12% for  $J^\pi \leq 1^\pm$ .

Table XVI displays the  $J \leq 2$  HDD and DISP2 results which determine the final outcome of this investigation. Note especially that the DISP2 results displayed in Table XVI include all of the appropriate  $(NN)\Delta$  channels, not just the  $^1S_0(NN)$   $\Delta$ -spectator channel as in Table XIV. The inferred  $\Delta\Delta$  3BFE is given in the last column of the table. The net results in the final row of Table XVI are not calculated results, but are obtained by combining the calculated results which appear above them in the table. Because the contribution of the  $J^\pi=2^+$  channels (determined by comparing the first and third rows of Table XVI) is small, this contribution is treated as a perturbation and is simply added by hand to the computed results presented in the second row of the table in order to obtain the net results of the final row of Table XVI. The predicted  $\Delta\Delta$  3BFE is, at 500 keV, substantial. The  $J^\pi=2^-$  channels contribute about 190 keV to this figure, while the  $J^\pi=2^+$  channels' contribution is only about 20 keV. The  $\Delta\Delta$  3BFE, though large, is about a factor of 2 smaller than the corresponding 920 keV one- $\Delta$  3BFE found in Ref. [1]. It is tempting to attribute this to the fact that the  $\Delta\Delta$  3BF diagrams of Fig. 3 require an additional iteration of the Faddeev equation to couple back to the dominant  $NNN$  sector as compared to the one- $\Delta$  3BF

TABLE XVI. Full  $J \leq 2$  HDD and DISP2 results (in MeV) for the triton binding energy;  $L(N\Delta)$ ,  $L(\Delta\Delta) \leq 2$ . The last column gives the net  $\Delta\Delta$  three-body force effect exhibited by the corresponding HDD calculation, in keV. Results in the last row, labeled with an asterisk, are not computed results but are obtained by combining the results located above them. The number of three-body channels in the calculations is indicated parenthetically.

Channels	HDD	DISP2	$\Delta\Delta$ 3BFE
$J \leq 1, \pi = \pm$	6.67(44)	6.38(21)	290
$J \leq 1, \pi = \pm; J = 2, \pi = -$	7.15(72)	6.67(37)	480
$J \leq 1, \pi = \pm; J = 2, \pi = +$	6.84(80)	6.53(35)	310
$J \leq 2, \pi = \pm, *$	7.32*(108)	6.82*(51)	500*

diagram of Fig. 1, so that the  $\Delta\Delta$  3BFE depends on the product of two relatively small amplitudes whereas the one- $\Delta$  3BFE depends on only one relatively small three-body amplitude:  $(N\Delta)N$ . However, there are five distinct lowest-order  $\Delta\Delta$  3BF diagrams (Fig. 3) as opposed to only one one- $\Delta$  diagram (Fig. 1). Also, this analysis may not be adequate for the Hannover  $\Delta\Delta$  model because trinuclear  $\Delta\Delta$  components are at  $\sim 5\%$ , relatively large. In fact, if one restricts attention to the  $\Delta\Delta$  model itself, then the one- $\Delta$  3BFE (defined in this case as the difference between DISP2 and  $\Delta\Delta$  DISP1 calculations) is at 590 keV not much larger than the 500 keV  $\Delta\Delta$  3BFE. That this may be the relevant comparison is emphasized by comparing Figs. 4(a) and 4(b): the same  $\Delta\Delta$ -model two-body  $NN$ - $N\Delta$  amplitudes appear in both the one- $\Delta$  and  $\Delta\Delta$  3BF diagrams.

Because the 6.82 MeV (51-channel) DISP2 figure in Table XVI includes all of the appropriate  $(NN)\Delta$  channels, the correct number with which to compare it in order to obtain the added  $J \leq 2$  dispersive effect of the  $\Delta\Delta$  model is the 49-channel HB1\* result of Ref. [1], 7.75 MeV, which also includes all of the appropriate  $(NN)\Delta$  channels. This yields an added  $J \leq 2$   $\Delta\Delta$  dispersive effect of 930 keV.

The essence of the  $J \leq 2$  results of Table XVI is then that the net  $\Delta$ -induced dispersive effect of about 1480 keV (550 keV from the one- $\Delta$  model and an additional 930 keV from the  $\Delta\Delta$  model) is almost exactly cancelled

by the net 3BFE of about 1420 keV (920 keV from the one- $\Delta$  model, based on the 49-channel result of Ref. [1] which includes  $\Delta$ -spectator effects, and 500 keV from the  $N\Delta\Delta$  channels). This leaves the net  $J \leq 2$ ,  $L(N\Delta)$ ,  $L(\Delta\Delta) \leq 2$ , binding-energy prediction of Table XVI,  $E_T = 7.32$  MeV, very close to the corresponding Paris nucleons-only value of 7.38 MeV.

To obtain the final,  $J \leq 4$ ,  $L(N\Delta)$ ,  $L(\Delta\Delta) \leq 4$  prediction for  $E_T$ , one needs only to add the  $\Delta E_T(3,4)$  correction for the truncation of  $J=3,4$  and  $L(N\Delta)$ ,  $L(\Delta\Delta)=3,4$  channels, as given by Eq. (23), to the 7.32 MeV figure of Table XVI. To obtain the  $J=3,4$   $\Delta\Delta$  portion of the correction in Eq. (23), compare the 7.32 and 6.67 MeV HDD figures in Table XVI with the corresponding HB1\* figures of Ref. [1], 7.75 MeV (49-channel) and 7.06 MeV (21-channel), respectively. This yields a difference of 430 keV for  $J^\pi \leq 2^\pm$  and 390 keV for  $J^\pi \leq 1^\pm$ . The net  $J=2$   $\Delta\Delta$  contribution is thus only 40 keV, so that the  $J=3,4$   $\Delta\Delta$  correction in Eq. (23), which is  $\frac{1}{10}$  of this, is essentially zero. Adding the resultant correction  $\Delta E_T(3,4) = 110$  keV to the 7.32 MeV figure gives the final  $J \leq 4$  result for  $E_T$  as 7.43 MeV, which is to be compared to the corresponding nucleons-only prediction based on the Paris potential, 7.46 MeV. Thus  $\Delta$  effects basically cancel, leaving the purely nucleonic prediction for the triton binding energy largely intact.

## V. SUMMARY

This paper examines one- $\Delta$  and  $\Delta\Delta$  effects on the triton binding energy,  $E_T$ , within the Hannover  $\Delta$  models. Based on the one- $\Delta$  results of the previous paper in this series [1] and the trends observed in the investigations of this paper, trinuclear  $\Delta\Delta$  studies can be safely restricted to two-body total angular momentum  $J \leq 4$ , and two- and three-body channels with  $J=3,4$  and total orbital angular momentum  $L(N\Delta)$ ,  $L(\Delta\Delta) \geq 3$  can be neglected. Similarly, the trends of this paper in comparison with the one- $\Delta$  trends of the previous paper indicate that the truncation of the remaining  $N\Delta\Delta$  channels with  $J=3,4$  is also warranted, subject only to a small correction: the influence of  $\Delta\Delta$  dispersive effects on the contribution of the  $J=3,4$   $NNN$  channels is found to be only 10 keV, but an estimate of the added  $J=3,4$  ( $\Delta + \Delta\Delta$ ) three-body-force effect (3BFE) of the  $\Delta\Delta$  model cancels this, so that the net  $J=3,4$   $\Delta\Delta$  correction is negligible. This indicates that another result of the previous paper, that the attractive contribution to  $E_T$  from  $J=3,4$   $NNN$  and  $NN\Delta$

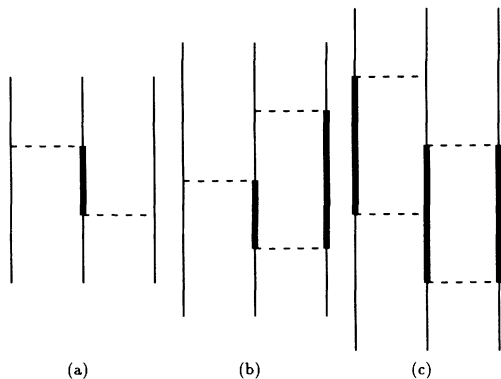


FIG. 4. Representative one- $\Delta$ ,  $\Delta\Delta$ , and  $\Delta\Delta\Delta$  3BF diagrams involving the fewest possible interactions, or steps. The one- $\Delta$ ,  $\Delta\Delta$ , and  $\Delta\Delta\Delta$  diagrams require two, three, and four steps, respectively.

channels (in that model  $\sim 140$  keV) can be added by hand as a correction to the results of  $J \leq 2$  calculations, can be extended to these  $\Delta\Delta$  studies and  $N\Delta\Delta$  channels as well. Thus the  $\Delta\Delta$  studies of this paper focus on  $J \leq 2$ , with a net attractive  $J=3,4$  correction of 140 keV.

The previous paper also established that, to within a repulsive 20 keV contribution, the  $J \leq 2$ ,  $L(N\Delta)=3,4$  channels' contribution to  $E_T$  is well represented in  $J \leq 1$  calculations. In this paper, the full  $J \leq 1$  contribution from channels with  $L(N\Delta)$ ,  $L(\Delta\Delta)=3,4$  is found to be a repulsive effect of only 10 keV. Moreover, the 20 keV correction is found to persist in full  $J \leq 2$  one- $\Delta$  calculations which incorporate all  $\Delta\Delta$  effects except those from  $N\Delta\Delta$  three-body channels. Because  $L(\Delta\Delta)=3,4$  effects are found to be uniformly small, any small 3BF contribution from  $L(\Delta\Delta)=3,4$   $N\Delta\Delta$  channels with  $J=2$  is neglected. The net  $J \leq 2$  and  $L(N\Delta)$ ,  $L(\Delta\Delta)=3,4$  (repulsive) correction to  $E_T$  is, thus, only 30 keV. The sum of all these truncations and associated corrections allow attention to be focused on the  $J \leq 2$  and  $L(N\Delta)$ ,  $L(\Delta\Delta) \leq 2$  channels, with a net (attractive) correction of only 110 keV due to these channel truncations.

Hannover-type,  $J \leq 2$ , one- $\Delta$  three-body calculations which use the two-body interaction of the  $\Delta\Delta$  model are found to exhibit an increased dispersive effect of 880 keV. This is substantially smaller than the 1.3 MeV perturbative estimate of the original Hannover calculations.

Full  $\Delta\Delta$ -model calculations for  $J \leq 1$  and  $L(N\Delta)$ ,  $L(\Delta\Delta) \leq 2$  are used to study the important mechanisms and correlations introduced into the trinuclear problem by the  $\Delta\Delta$  degrees of freedom. Consistent with the structure of the Faddeev equation,  $(N\Delta)\Delta$  channels are found to function as a doorway for  $\Delta\Delta$ -induced 3BF effects. Absent  $(N\Delta)\Delta$  channels, there is no 3BFE. For the doorway to be open for the important lowest-order  $\Delta\Delta$  3BF diagrams, however,  $(N\Delta)\Delta$  and  $(NN)\Delta$   $\Delta$ -spectator channels with the same pair  $(J^\pi, T)$  must both be present. The diagram of Fig. 3(c) is the only exception to this rule. Because of the doorway mechanism,  $\Delta$ -spectator channels must be included as an integral part of  $\Delta\Delta$  studies; they cannot be included as an afterthought, as was found possible in one- $\Delta$  studies. The net  $\Delta\Delta$  3BF contribution found in these restricted  $J \leq 1$  calculations is 290 keV of attraction, by itself about a factor of 3 larger than the total  $\Delta\Delta$  3BF contribution found in the Hannover perturbative calculations. This difference is attributed to the fact that the strictures of the perturbative calculations of Ref. [3] left the doorway largely closed.

The final component of these investigations is the extension of the full  $\Delta\Delta$ -model calculations to  $J \leq 2$  with  $L(N\Delta)$ ,  $L(\Delta\Delta) \leq 2$ . For reasons of economy this full calculation is not performed in a single step. Rather, the system is first reduced by eliminating the  $J^\pi=2^+$  channels and the resultant full  $\Delta\Delta$  calculation is performed. To the result of this calculation is added the effect of the  $J^\pi=2^+$  channels, which is itself determined by comparing the result of the full  $J \leq 1$   $\Delta\Delta$  calculation with a full  $\Delta\Delta$  calculation which includes both the  $J \leq 1$  and the  $J^\pi=2^+$  channels. Because the observed 20 keV attractive effect of the  $J^\pi=2^+$  channels is small, this procedure is expected to be especially dependable. The net result

for the  $\Delta\Delta$  3BFE is 500 keV of attraction, with 190 keV of this attributable to the  $J^\pi=2^-$  channels, while the added dispersive effect of the  $\Delta\Delta$  model is found to be 930 keV, and the corresponding net  $J \leq 2$  prediction for the triton binding energy is  $E_T=7.32$  MeV.

At 500 keV, the  $\Delta\Delta$ -induced 3BFE is substantial. It is reduced from the corresponding 920 keV one- $\Delta$  3BFE of the one- $\Delta$  model [1] by only about a factor of 2. It is tempting to ascribe this reduction to the way the two 3BF effects are produced by the Faddeev equation, as depicted diagrammatically in Fig. 4. In diagram 4(b) it takes one iteration of the Faddeev equation to generate  $(\Delta\Delta)N$  channels from the dominant  $NNN$  three-body channels, and two iterations for these  $(\Delta\Delta)N$  channels to couple back and affect the  $NNN$  channels. As a consequence, this  $\Delta\Delta$  3BFE depends on two relatively small Faddeev amplitudes:  $(\Delta\Delta)N$  and  $(NN)\Delta$ . In contrast, in diagram 4(a)  $(N\Delta)N$  channels are also generated by one iteration of the Faddeev equation, but they couple back to the  $NNN$  sector after only one iteration as well. Thus the one- $\Delta$  3BFE depends on only one relatively small Faddeev amplitude:  $(N\Delta)N$ . However, there are five lowest-order  $\Delta\Delta$  3BF diagrams as opposed to one one- $\Delta$  diagram. Also, because of the appreciable  $\Delta\Delta$  component found in the model ( $\sim 5\%$ ), this analysis may not be adequate for the Hannover  $\Delta\Delta$  model. In fact, the one- $\Delta$  3BFE of the  $\Delta\Delta$  model itself [defined as the difference between three-body  $(NNN + NN\Delta)$  calculations and  $NNN$  calculations, both calculations using  $\Delta\Delta$ -model, two-body amplitudes] is 590 keV. This figure differs little from the 500 keV  $\Delta\Delta$  3BFE.

Because the  $\Delta\Delta$  3BFE is so much larger than that found by the Hannover perturbative calculations, the present results do not support the conclusion of Ref. [3] that the net 3BFE can be considered established at the  $\Delta\Delta$  level. Moreover, because there is no further dispersive effect associated with the inclusion of  $\Delta\Delta\Delta$  channels, any  $\Delta\Delta\Delta$ -induced 3BFE directly translates into a shift in the prediction for  $E_T$ . Following the line of the discussion above, and with reference to Fig. 4, it takes two iterations of the Faddeev equation to generate  $\Delta\Delta\Delta$  channels from the dominant  $NNN$  sector, and two iterations to couple back to the  $NNN$  sector. As a consequence,  $\Delta\Delta\Delta$  3BF effects depend both on two relatively small Faddeev amplitudes and on weakly coupled  $\Delta\Delta\Delta$  components. Thus  $\Delta\Delta\Delta$  3BF effects may be expected to be reduced from the  $\Delta\Delta$  figure of 500 keV. However, judging by the differences between the one- $\Delta$  and  $\Delta\Delta$  figures in either of the cases described in the preceding paragraph (there are sixteen distinct lowest-order  $\Delta\Delta\Delta$  3BF diagrams as compared with the five  $\Delta\Delta$  diagrams), the  $\Delta\Delta\Delta$  3BF contribution need not be negligible.

The most important outcome of the  $J \leq 2$  and  $L(N\Delta)$ ,  $L(\Delta\Delta) \leq 2$  results is the essential cancellation of all one- $\Delta$  and  $\Delta\Delta$  contributions to  $E_T$ . The total  $\Delta$ -induced dispersive effect is 1480 keV (a 550 keV one- $\Delta$ -model effect and an additional 930 keV from the  $\Delta\Delta$  model), which almost exactly cancels against the total  $\Delta$ -induced 3BFE of 1420 keV (920 keV from the one- $\Delta$  model and an additional 500 keV  $\Delta\Delta$  3BFE). This cancellation leaves the corresponding nucleons-only prediction for  $E_T$  based on the

Paris potential largely intact. For example, the full  $J \leq 2$   $\Delta\Delta$ -model result for  $E_T$  is, at 7.32 MeV, very close to the corresponding nucleons-only result of 7.38 MeV. Adding to this 7.32 MeV figure the net correction of 110 keV for the truncated channels [the sum of the  $J=3,4$  correction and the  $J \leq 2$  and  $L(N\Delta)$ ,  $L(\Delta\Delta)=3,4$  correction] yields a net  $J \leq 4$  and  $L(N\Delta)$ ,  $L(\Delta\Delta) \leq 4$   $\Delta\Delta$ -model result for the triton binding energy of  $E_T=7.43$  MeV; the corresponding nucleons-only result is  $E_T=7.46$  MeV.

Qualitatively, these results obviously entail important implications for both nucleons-only nuclear physics and attempts to reconcile the theoretical prediction of  $E_T$  with its actual physical value. For example, leading corrections to the nucleons-only picture of nuclear physics unexpectedly cancel in  $E_T$ , leaving the nucleons-only picture largely intact, and although the triton binding energy defect is not ameliorated by the incorporation of  $\Delta$  and  $\Delta\Delta$  degrees of freedom, at least it is not worsened substantially as was previously thought to be the case. However, a critical examination of the two-body performance of the Hannover  $\Delta\Delta$  force model (see Sec. III) in-

dicates appreciable defects, particularly in the  $^1S_0(NN)$  channel. These defects introduce a degree of uncertainty in regard to the physical relevance of quantitative results based on the Hannover  $\Delta\Delta$  model. In addition, the schematic nature of the Hannover  $\Delta\Delta$  model entails the neglect of requisite repulsive interactions within the  $N\Delta$  and  $\Delta\Delta$  two-body channels. Such interactions tend to reduce  $\Delta$ -induced effects. These caveats notwithstanding, these qualitative results, especially the large cancellations observed, may be of more general validity than the specific model used to obtain them. Nevertheless, the implications of these qualitative, three-body results are dependent on confirmation from three-body calculations based on a more sophisticated force model. Thus the next paper in this series carries out a corresponding investigation using the Argonne V-28 force model. Of course, also yet to be investigated are  $\Delta\Delta\Delta$  contributions to  $E_T$ , as well as contributions from "exotic" two-body channels [ $N\Delta$  and  $\Delta\Delta$  channels decoupled from the  $NN$  sector:  $T=2$  channels and other channels in non-nucleonic ( $J^\pi, T$ ) sectors].

- 
- [1] A. Picklesimer, R. A. Rice, and R. Brandenburg, *Phys. C* **44**, 1359 (1991).
- [2] Ch. Hajduk, P. U. Sauer, and W. Strueve, *Nucl. Phys.* **A405**, 581 (1983).
- [3] Ch. Hajduk, P. U. Sauer, and S. N. Yang, *Nucl. Phys.* **A405**, 605 (1983).
- [4] R. B. Wiringa, R. A. Smith, and T. L. Ainsworth, *Phys. Rev. C* **29**, 1207 (1984).
- [5] M. Lacombe, B. Loiseau, J. M. Richard, R. Vinh Mau, J. Côté, P. Pirès, and R. de Tournel, *Phys. Rev. C* **21**, 861 (1980).
- [6] M. T. Peña, H. Henning, and P. U. Sauer, *Phys. Rev. C* **42**, 855 (1990).
- [7] B. F. Gibson and G. J. Stephenson, Jr., *Phys. Rev. C* **8**, 1222 (1973).
- [8] R. A. Brandenburg, G. S. Chulick, R. Machleidt, A. Picklesimer, and R.M. Thaler, *Phys. Rev. C* **37**, 1245 (1988).
- [9] A. R. Edmonds, *Angular Momentum in Quantum Mechanics* (Princeton University Press, Princeton, NJ, 1957).